Biochimica et Biophysica Acta, 974 (1989) 81–87
Elsevier

BBA 42962

Refined analysis of the trimeric structure of the isolated Photosystem I complex from the thermophilic cyanobacterium *Synechococcus* sp.

E.J. Boekema [1,*], J.P. Dekker [2], M. Rögner [2], I. Witt [3], H.T. Witt [2] and M. van Heel [1]

[1] *Fritz-Haber-Institut der Max-Planck-Gesellschaft,* [2] *Max Volmer Institut, Technische Universität Berlin and* [3] *Institut für Kristallographie, Freie Universität Berlin, Berlin (Germany)*

(Received 14 June 1988)
(Revised manuscript received 30 November 1988)

Key words: Photosystem I structure; Electron microscopy; Image analysis; (*Synechococcus*)

The trimeric structure previously evaluated from isolated Photosystem I (PS I) reaction-center complex of the thermophilic cyanobacterium *Synechococcus* sp. was studied in more detail by electron microscopy and computer image analysis. Molecular projections (1970 top views and 457 side views) were selected from electron micrographs and subsequently aligned to different references. The top views were submitted to a multivariate statistical classification procedure. Two types of top view, which differ in handedness and represent face-up and face-down oriented molecules, could be separated. The classification shows that the PS I trimeric complex consists of three very similar, if not identical, units. The trimer has the shape of a disk with a diameter of 19 nm and a thickness of 6.5 nm. The monomers within the trimer have an asymmetric shape. Possible arrangements of the two major subunits within the monomer are discussed.

Introduction

Light-induced charge separation in the reaction centers of Photosystem I (PS I) leads to the oxidation of a special chlorophyll *a* molecule Chl *a*I (P-700) and to the sequential reduction of a number of electron acceptors (see Refs. 1 and 2 for reviews). The primary electron acceptors are probably a Chl *a* molecule absorbing at 693 nm [3] and a phylloquinone [4–8]. Under physiological conditions, with certainty, the next acceptor is an iron-sulfur center called F_X (A2), interpreted by Golbeck et al. [9] as a [2Fe-2S] cluster. The terminal acceptors of PS I are two interacting [4Fe-4S] centers called F_A and F_B.

In the reaction-center complex, the pigment molecules and the redox centers between Chl *a*I and F_X are located in one or two integral membrane proteins with apparent molecular masses (based on SDS-PAGE) of about 64 kDa [10,11]. Recently, a '64 kDa' and a '56 kDa' subunit were identified as products from the *psa-B* and *psa-A* genes, respectively [12]. In maize, these genes were sequenced and found to code for 82.5 and 83.2 kDa subunits, containing 735 and 751 amino acids respectively [13,14]. For the cyanobacterium *Synechococcus* PCC 7002, large parts of the sequences have been reported as well [15]; these genes are 78–84% homologous with their maize counterparts. In addition to the *psa-A* and *psa-B* gene products, the cyanobacterial PS I reaction center contains four subunits in the range of 9–18 kDa [16]. One or more of these subunits are involved in the binding of the iron-sulfur centers F_A and F_B [17,18].

Further information on the structure and shape of the PS I complex is relatively scarce. However, the recent success in the crystallization of the PS I complex [19,20] may change this situation dramatically in the future. By using electron microscopy, Williams et al. [21] analyzed Triton X-100-solubilized PS I particles with the negative-staining technique and found ellipsoid particles of about 18×8 nm. Recently, we reported on the purification and characterization of PS I reaction-center complexes from the cyanobacterium *Synechococcus* sp. by using the detergents Sulfobetain 12 and β-dodecylmaltoside. It was shown by HPLC gel filtration that due to the use of these relatively mild detergents the preparation consists of a homogeneous population of particles with a molecular mass of about 600

* Current address: Biochemisch Laboratorium, Rijksuniversiteit Groningen, Nijenborgh 16, 9747 AG Groningen, The Netherlands.

Correspondence: M. van Heel, Fritz Haber Institute of the Max Planck Society, Faradayweg 4–6, 1000 Berlin 33, Germany.

kDa. We showed by electron microscopy and image analysis that these isolated particles have the structure of a trimer with a disk-like form [22]. In this paper we report on the detailed characterization of these particles by electron microscopy and multivariate statistical analysis. After aligning a large set of molecular images relative to each other, multivariate statistical-classification techniques can be used to find similar images in the mixed data set; 'face-up' and 'face-down' differences were detected in a number of cases such as for hemocyanin molecules [23].

Materials and Methods

Cells and membranes of the thermophilic cyanobacterium *Synechococcus* sp. were grown as in Ref. 24 and prepared as in Ref. 25. PS II was removed from the membranes with the zwitterionic detergent Sulfobetain 12 (usually 0.3–0.4%) according to Ref. 25. PS I was extracted from the pellet by a similar treatment but now with 0.8–1.1% Sulfobetain 12, and further purified by sucrose-density centrifugation and ion-exchange chromatography as described in Ref. 22. The isolated particles contain six different subunits ([22] and [33]), with masses similar to those in Ref. 16. Absorption-change activity measurements with benzyl viologen as acceptor indicate that the preparation still contains the iron-sulfur centers F_A and F_B [20].

Specimens for electron microscopy were prepared by the droplet method, using 1% uranyl acetate as a negative stain. For electron microscopy the purified PS I samples were diluted in buffer plus 1.1% octyl glucopyranoside. Electron microscopy was carried out on a Philips EM 300 or 400T microscope at 70 000 × magnification. Selected micrographs were digitized with a Datacopy Model 610F electronic digitizing camera (Datacopy, Long Beach, CA, U.S.A.). The scanning step used was 32 μm, corresponding to a pixel size of 0.47 nm on the specimen level. Image analysis was performed by means of the IMAGIC software system [26] on a VAX 780 computer. All images were band-pass filtered to remove the very high (greater than $(1.2\ \text{nm})^{-1}$) and suppress the very low (less than $(12\ \text{nm})^{-1}$) frequency components. The very low frequency components are normally related to stain gradients in the environment of the molecule and are not structure-related [28]. The next steps in the analysis – alignment of the images, the eigenvector-eigenvalue data compression procedure ('correspondence analysis') and the automatic classification – were carried out as described previously [27–30].

Results

In general, it is difficult to obtain well-preserved samples of membrane proteins by negative staining, since the hydrophobic parts of these molecules are stain-excluding. Moreover, detergent molecules, which are necessary to keep the particles in a monodisperse solution, give rise to a strong background on the specimen. A low detergent concentration, however, leads either to PS I molecules aggregated into large sheets, as was also noticed by Williams et al. [21], or to randomly clustered material. The best compromise for making good specimens is to add detergent to the buffer solution in a concentration of about 2–3-times the critical micellar concentration during preparation. Before staining the grid, a large amount of the detergent is removed by quickly washing with distilled water. Fig. 1 illustrates that by following this staining procedure it is possible to obtain clear images of PS I particles in the presence of octylglucopyranoside. β-Dodecylmaltoside gives similar results, but causes a higher background because it forms larger detergent micelles.

Inspection of the micrographs shows that there are two typical projections of the solubilized particles: an almost circular top view and an elongated side view. If particles are lying on their sides, they frequently aggregate as a 'stack of coins'. A small cleft filled with negative stain between the particles always characterizes such aggregates. Other purified photosynthetic membrane proteins can aggregate in a very similar way [25,31].

Analysis of top-view projections

From 38 digitized micrographs 1970 top-view projections were selected (Fig. 2) to ensure good statistical significance of the results. The projections were brought into register by repeated alignments on improving references [28,30]. After the first alignment cycle, we noticed that the total sum of all particles showed a nearly three-fold symmetry, but had a clear handedness (i.e., departure from mirror symmetry). To avoid biasing the data set towards one particular reference image [30], in casu, towards a left- or a right-handed projection of the molecule, each reference image in the multi-reference alignment procedure [28] was also used in its mirrored version [32].

In the next step, the data set was classified with a multivariate statistical algorithm [29]. The classification not only facilitates the discrimination of principally different views but also allows one to judge the quality of the particles. The treated data set was partitioned into 14 classes, and the members of each class (roughly 100 per class) were summed in order to enhance the signal-to-noise ratio. During the classification, 24% of the projections were automatically rejected based on their large contribution to the variance of the data set [28]. The 14 classes are shown in Figs. 3A–N. One sees that the classification resulted in a separation of the projections into two different types, which are roughly mirror-related. These types represent the two ways the

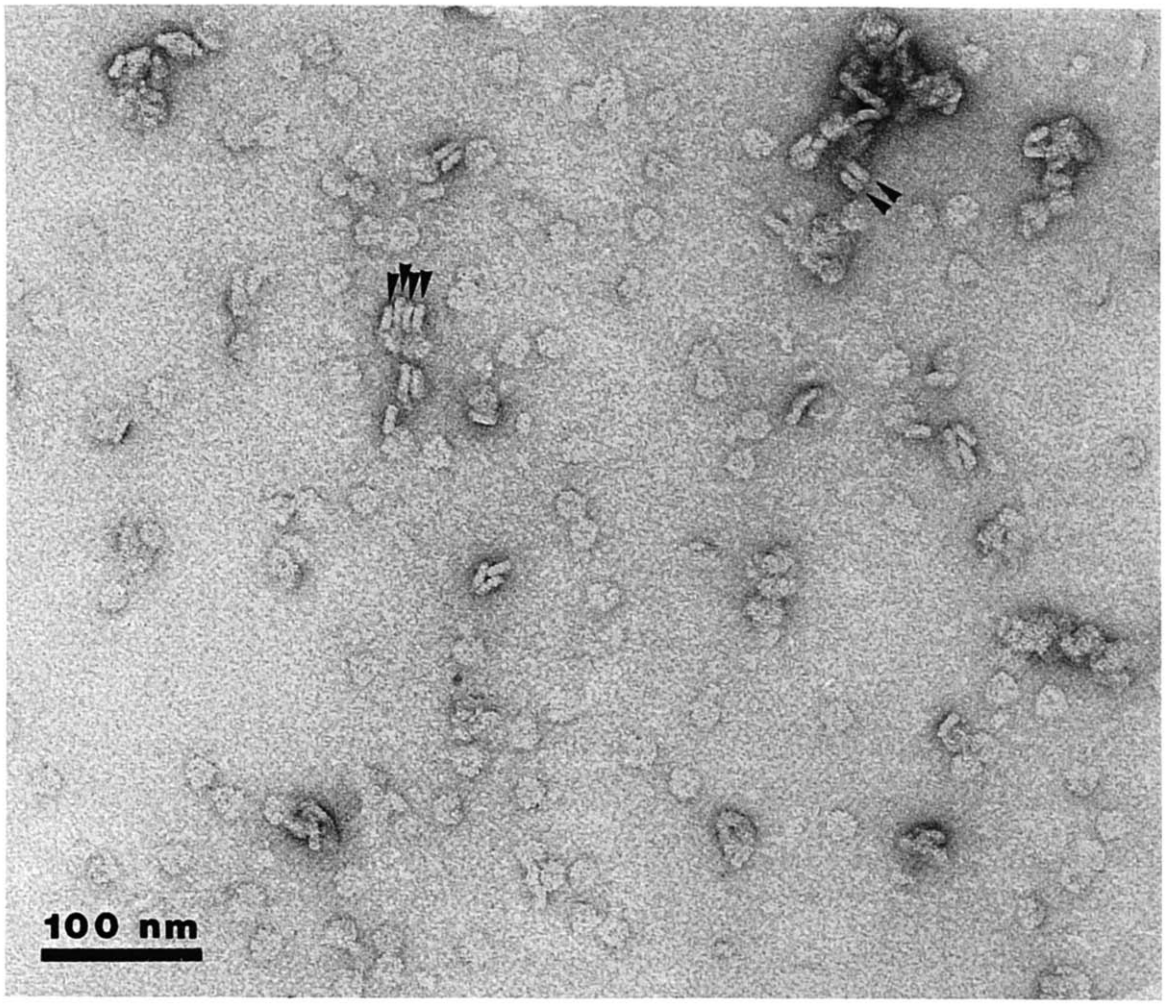

Fig. 1. Electron micrograph of PS I particles, negatively stained with 1% uranyl acetate in the presence of 1.1% octyl glucopyranoside. Arrowheads, indicate side-view stacks of the particles.

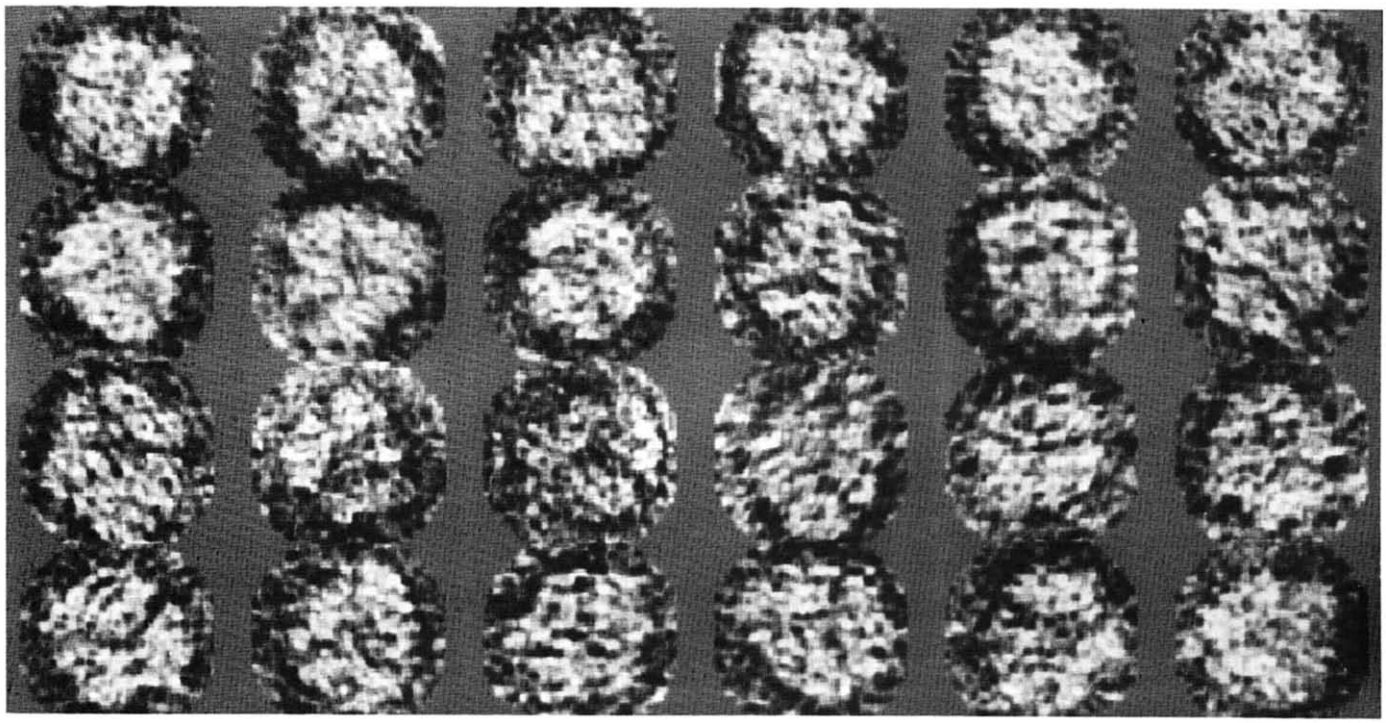

Fig. 2. A gallery of 24 digitized top-view projections (out of 1970) used for image analysis.

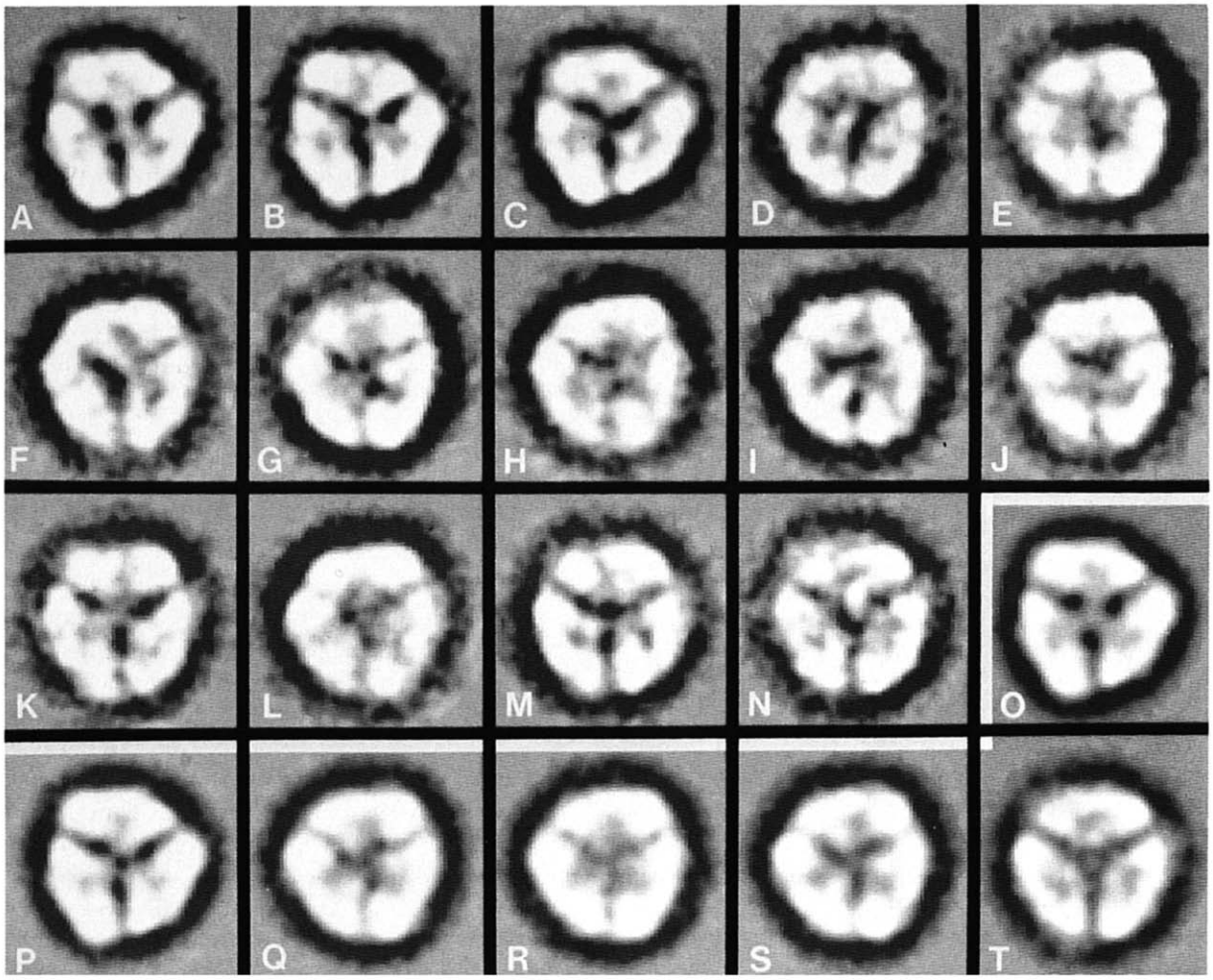

Fig. 3. Classification of the top-view projections. The images of the 14 classes A–N represent the sums of 137, 127, 137, 94, 115, 102, 109, 99, 104, 105, 95, 101, 103 and 74 projections, respectively. Figs. O–T are the three-fold-averaged images of classes A, B, G, H, I and N, respectively. The motif of the monomer, in the shape of a 'shoe', is clockwise oriented in classes A–C (see also O and P for three-fold-averaged versions) and counterclockwise oriented in D–L and three-fold-averaged versions in Q–S. No handedness is visible in Figs. 3M–N and the averaged version 3T. Note: the images are shown with imposed band-pass filter which is necessary for the suppression of unwanted noise during analysis. This filter allows a better analysis of the features, but has the disadvantage of suppressing the central density (see also Fig. 4).

molecules can be attached to the carbon support film ('face-up' and 'face-down'). One type is found in three classes having a total of 401 projections (Figs. 3A–C), the other type in about nine classes (Fig. 3D–L) with 924 projections. The motif of the monomer has roughly the shape of a 'shoe'; and if we focus on this motif we can see that the three 'shoes' of the trimer are oriented either clockwise (arbitrarily defined as 'face-up' or 'left-handed', Figs. 3A–C) or counterclockwise ('right-handed' or 'face-down', Figs. 3D–L), with clearest examples in Figs. 3G–I. The presence of a handedness is easier to see if the trimers are three-fold averaged, and therefore six classes are also shown in their three-fold-symmetrized version. Figs. 3O and 3P shows three-fold-average version of A–B (clockwise); Figs. 3Q–S show averaged version of D–L (counterclockwise). In some classes, especially those of Figs. 3M–N, with a total of 177 members, the handedness is impossible to determine: in Fig. 3T, which is the three-fold-averaged version of 3N, the 'shoe' has no clear direction at all. It is likely that these classes 3M–N contain a mixture of both types of projection as well as badly aligned and/or damaged molecules.

In principle, the ratio between the two types of top-view should be 1 : 1 if the attachment to the support is just a random process. Since the ratio is about 2 : 1, there apparently is some preference in the way the molecular stick to the support, which might originate from charge differences between the face-up and face-down sides of the particles [13]. Interestingly, in the type with the smallest number of classes (Figs. 3A–C) the features of the object seem to have been slightly better outlined. Therefore, these 401 images were re-aligned on the image of Fig. 3A and were taken together to give a final result for the top-view analysis. Fig. 4 shows this sum with its original spatial frequency components restored (clockwise version).

The outer regions of the molecules, as seen in the

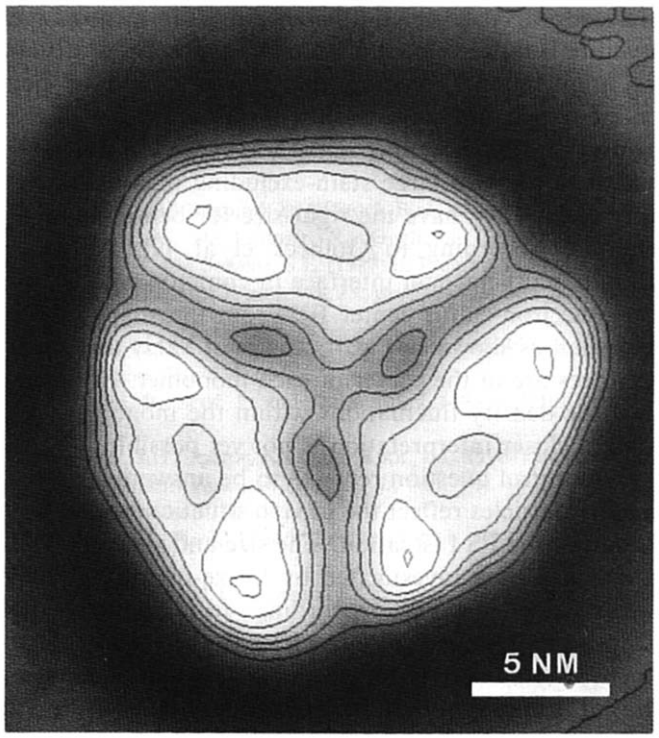

Fig. 4. Average of the 401 left-handed top-view projections from Figs. 3A–C, summed after re-alignment of the original projections. The image is countered with equidistant contour levels.

top-view projection, must have a hydrophobic surface. Lowering the detergent concentration leads to molecules clustered in extensive two-dimensional sheets of about the same thickness as individual trimers in the top-view projection (results not shown). To keep the particles in a monodisperse solution, a boundary layer of detergent is expected to surround the molecules. Since detergent is strongly stain-excluding, the top views consist of the actual PS I particle plus the boundary layer. The image analysis was carried out on trimers prepared in the presence of octyl glucoside. This results in a diameter of 19 nm. The diameter of particles isolated and prepared for electron microscopy in the presence of the larger detergent β-dodecylmaltoside is 22–23 nm on the average. This further confirms the supposition that the outer edges of the trimer in top-view projection are formed by the detergent boundary layer.

Analysis of side-view projection

A total of 457 side-views were aligned and summed together in order to get an impression of the thickness of the PS I particle. The average image (Fig. 5A) is clearly outlined by the negative stain. However, internal features are lacking because the image is made by averaging (rotationally) different projections. The dimensions of the sum of all 457 side-view projections were found to be 19 and 6 nm (Fig. 5A). They depend, however, on the surrounding of the particles: the amount of attached negative stain and the influence of neighboring molecules. A minor number of 35 particles is lying free on the carbon support. They appear to be slightly thicker: 6.7 nm (see Fig. 5B) due to tilting freedom in this position.

The width for particles lying in close contact with others (Fig. 5C) is 6.5 nm, measured as the distance between the two stain maxima on both sides of the side view. This value is the most accurate estimation for the

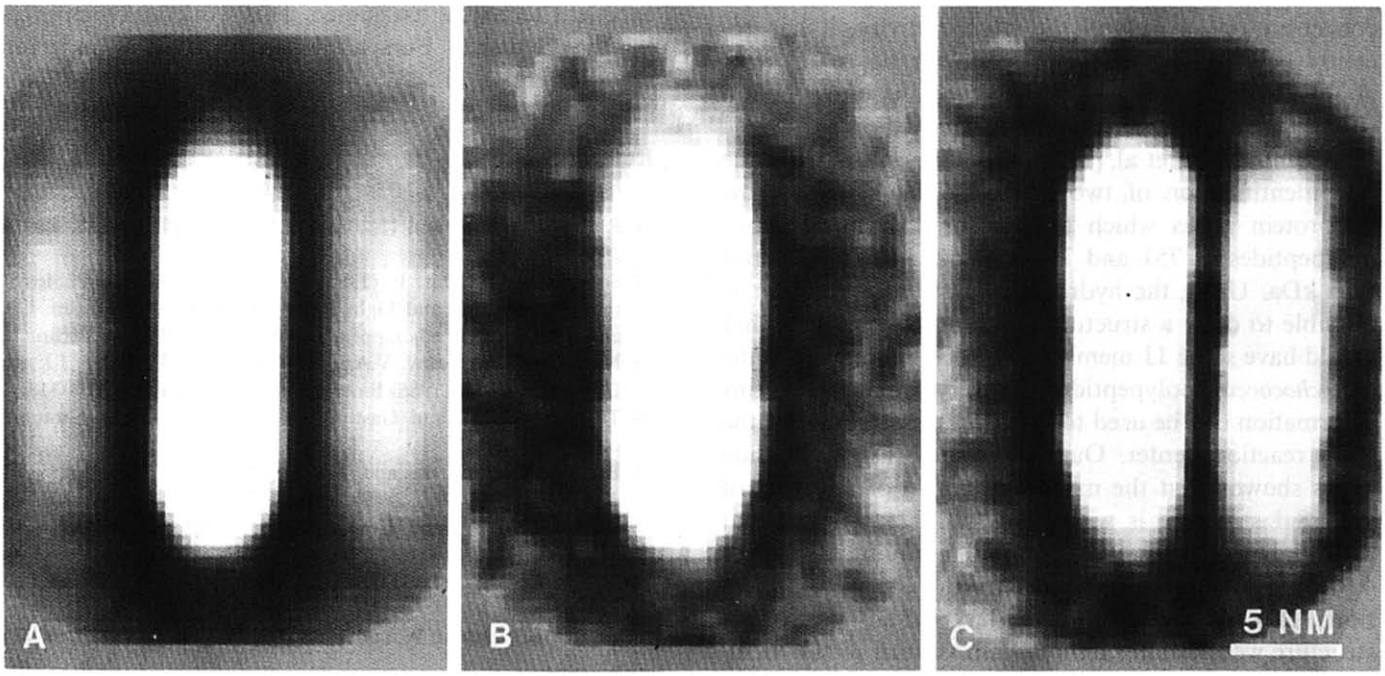

Fig. 5. Size analysis of side-view projections. A, average image of all 457 particles that were well-aligned; B, average image of 35 particles not in contact with others; C, average image of 26 particles with one neighbor closely associated.

width, since particles are in close contact with others and have less tilting freedom.

Discussion

In this paper we have presented further information on the trimeric structure of the isolated PS I complex from the thermophilic cyanobacterium *Synechococcus* sp. The overall structure was found to be a circular disk with a diameter of about 19 nm and a thickness of 6.5 nm. Image analysis showed that the top-view projection has close to three-fold symmetry (Fig. 3, 4). Moreover, there are two types of top view, which differ in handedness and represent face-up and face-down oriented molecules. The three monomers could be identical, but this question cannot be answered from the present data alone. Since no departure from symmetry can be proven, we presented our final top-view sum (Fig. 4) with three-fold symmetry imposed.

The molecular mass of the PS I trimer, estimated from its dimensions and assuming a specific volume of $2 \pm 0.5 \cdot 10^{-3}$ nm $\cdot$ Da^{-1}, is about 700–800 kDa, which is roughly in agreement with the apparent mass of 600 kDa from gel-filtration experiments [22]. Accordingly, the molecular mass of each monomer would be around 250 kDa. This is compatible with the view that the PS I reaction center consists of two large subunits and four smaller subunits (see previous sections). The protein part would then have a molecular mass of about 190 kDa. When the additional mass of chlorophylls, lipids and/or detergents is taken into account, an estimate of 250 kDa is not unrealistic. Through biochemical decomposition of the trimer into three monomers, together with the determination of the protein and chlorophyll concentration as well as the photo-activity, it has recently been shown that one monomer has a mass of about 260 kDa. Each monomer contains one reaction center Chl *a*I (Rögner et al., unpublished data).

Recently, Fish et al. [13,14] reported on the sequence and identification of two maize P-700 chlorophyll *a*-apoprotein genes which encode for 45% homologous polypeptides of 751 and 735 amino-acids, or 83.2 and 82.5 kDa. Using the hydropathy plots as a guide, it is possible to draw a structure for these polypeptides that would have some 11 membrane-buried helices. Since the *Synechococcus* polypeptides are very similar [15], this information can be used to interpret the structure of the PS I reaction center. Our image analysis of the side views showed that the maximum height of any part of the PS I structure is within 6.5 nm. This implies that these polypeptides must at least fill a minimum space of 4×5 nm in the plane as seen in the top-view projections. This space would be even larger if any part of the structure were thinner than 6.5 nm vertical to the membrane. The large hydrophilic regions in the sequence between the alpha-helical regions of the predicted structure lead one to conclude that presumably most of the structure is indeed about 6.5 nm in height. These structural implications constrain the interpretation of our top-view structure considerably. An examination of the features of each monomer in the top view (Fig. 4) shows that there are two large stain-excluding regions on the outer ends. They have the right size for being the large subunits. According to Golbeck et al. [9], the large subunits must have an interface in common where they share the iron-sulfur center F_x. From the shape of the monomer, as shown in Fig. 4, it is most likely that these interfaces are in the center of each monomer. However, since the density fluctuations within the monomers are small, a closer interpretation is not yet possible.

One central question remains to be answered: do the trimeric particles reflect the in vivo situation or are they a result of the PS I isolation? The size and shape of PS I in vivo has been investigated by freeze-fracturing techniques. For instance, according to Giddings and Staehelin [33], none of the particles in the thylakoids of *Anabena cylindrica* is larger than 10 nm in diameter. Thus, it is apparent that, in general, only monomeric PS I complexes exist in vivo in the membrane. It can, however, not be excluded that some specialized organisms, like this thermophilic *Synechococcus* cyanobacterium, may have their PS I aggregated into trimers. Work is in progress to clarify this point.

Acknowledgements

We thank Prof. E. Zeitler for his general support of the work, Dr. George Harauz for his contributions to the programming effort and Matina Gerdsmeyer for excellent technical assistance. This work was supported by the Deutsche Forschungsgemeinschaft (Sonderforschungsbereich 312).

References

1 Rutherford, A.W. and Heathcoate, P. (1985) Photosynth. Res. 6, 295–316.
2 Setif, P. and Mathis, P. (1986) in Photosynthesis III, Photosynthetic Membranes and Light Harvesting Systems (Steahelin, L.A. and Arntzen, C.J., eds.), pp. 476–486, Springer Verlag, Berlin.
3 Nuijs, A.M., Shuvalov, V.A., Van Gorkom, H.J., Plijter, J.J. and Duysens, L.N.M. (1986) Biochim. Biophys. Acta 850, 310–318.
4 Thurnauer, M.C. and Gast, P. (1985) Photobiochem. Photobiophys. 9, 29–38.
5 Brettel, K., Setif, R. and Mathis, P. (1986) FEBS Lett. 203, 220–224.
6 Mansfield, R.W. and Evans, M.C.W. (1986) FEBS Lett. 203, 225–229.
7 Palace, G.P., Franke, J.E. and Warden, J.T. (1987) FEBS Lett. 215, 58–62.
8 Ziegler, K., Lockau, W. and Nietschke, W. (1987) FEBS Lett. 217, 16–20.
9 Golbeck, J.H., McDermott, A.E., Jones, W.K. and Kurtz, D.M. (1987) Biochim. Biophys. Acta 891, 94–98.

10 Golbeck, J.H. and Cornelius, J.M. (1986) Biochim. Biophys. Acta 849, 16–24.
11 Hoj, P.B. and Moller, B.-L. (1986) J. Biol. Chem. 261, 14292–14300.
12 Margulies, M.M. and Tiffany, H.L. (1987) Biochem. Biophys. Res. Commun. 143, 281–287.
13 Fish, L.E., Kuck, U., Bogorad, L. (1985) J. Biol. Chem. 260, 1413–1421.
14 Fish, L.E. and Bogorad, L. (1986) J. Biol. Chem. 261, 8134–8139.
15 Bryant, D.A., De Lorimer, R., Gugliemi, G., Stirewalt, V.L., Cantrell, A. and Stevens, S.E. (1987) in Progress in Photosynthesis Research (Biggins, J., ed.), Vol. IV, pp. 749–755, Martinus Nijhoff, Dordrecht.
16 Lundell, D.J., Glazer, A.N., Melis, A. and Malkin, R. (1985) J. Biol. Chem. 260, 646–654.
17 Lagoutte, B., Setif, P. and Duranton, J. (1984) FEBS Lett. 174, 24–29.
18 Golbeck, J.H., Parrot, K.G. and Root, L.L. (1987) in Progress in Photosynthesis Research (Biggins, J., ed.), Vol. IV, pp. 749–755, Martinus Nijhoff, Dordrecht.
19 Ford, R.C., Picot, D.and Garavito, R.M. (1987) EMBO J. 6, 1581–1586.
20 Witt, I., Witt, H.T., Gerken, S., Saenger, W., Dekker, J.P. and Rögner, M. (1987) FEBS Lett. 221, 260–264.
21 Williams, R.C., Glazer, A.N., Lundell, D.J. (1983) Proc. Natl. Acad. Sci. USA 80, 5923–5926.
22 Boekema, E.J., Dekker, J.P., Van Heel, M.G., Rögner, M., Saenger, W., Witt, I. and Witt, H.T. (1987) FEBS Lett. 217, 283–286.
23 Bijlholt, M.M.C., Van Heel, M.G. and Van Bruggen, E.F.J. (1982) J. Mol. Biol. 161, 139–153.
24 Schatz, G.H. and Witt, H.T. (1984) Photobiochem. Photobiophys. 7, 1–14.
25 Rögner, M., Dekker, J.P., Boekema, E.J. and Witt, H.T. (1987) FEBS Lett. 219, 207–211.
26 Van Heel, M.G. and Keegstra, W. (1981) Ultramicroscopy 7, 113–130.
27 Van Heel, M.G. and Frank, J. (1981) Ultramicroscopy 6, 187–194.
28 Van Heel, M. and Stöffler-Meilicke, M. (1985) EMBO J. 4, 2389–2395.
29 Van Heel, M.G. (1984) Ultramicroscopy 13, 165–183.
30 Boekema, E.J., Berden, J.A. and Van Heel, M.G. (1986) Biochim. Biophys. Acta 851, 353–360.
31 Kühlbrandt, W., Thaler, T. and Wehrli, E. (1983) J. Cell Biol. 96, 1414–1424.
32 Harauz, G., Boekema, E.J. and Van Heel, M. (1988) Methods Enzymol. 164, 35–49.
33 Giddings, T.H. and Staehelin, L.A. (1979) Biochim. Biophys. Acta 546, 373–382.